Revista Geoaraguaia
ISSN:2236-9716
Barra do Garças – MT
v.10, n. esp. Geologia e
Pedologia p.06-32. Dez-2020

MINERAL CHEMISTRY OF FELDSPAR AND AMPHIBOLE APPLICATION OF DIFFERENT GEOTHERMOBAROMETRY METHODS AND OXYGEN FUGACITY, DETERMINATION OF MAGMATIC SERIES, ORIGIN AND TECTONOMAGMATIC CLASSIFICATION OF SHIRKUH GRANITOID BATHOLITH, YAZD, IRAN

QUÍMICA MINERAL DA APLICAÇÃO DE FELDSPATO E ANFIBÓLIO DE DIFERENTES MÉTODOS DE GEOTERMOBAROMETRIA E FUGACIDADE DO OXIGÊNIO, DETERMINAÇÃO DE SÉRIES MAGMÁTICAS, ORIGEM E CLASSIFICAÇÃO TECTONOMAGMÁTICA DO BATÓLITO GRANITÓIDE SHIRKUH, YAZD, IRÃ

Hripsimeh Az Mikaelians[1]

Afshin Ashja Ardalan[2]*

Seyed Jamal Sheikhzakariayi[3]

Shiva Ansari [4]

ABSTRACT

Batholith of Shirkuh, Yazd, is part of the central Iranian structural zone, located southwest of the province. The lithology of this complex comprises mostly monzogranite and granodiorite and some quartz monzonite, quartz monzodiorite and syenogranite.Plagioclase, quartz, orthoclase, biotite and amphibole are the dominant minerals in these rocks. The composition of plagioclases varies from labradorite to oligoclase, and alkali feldspars belong to the orthoclase category. Amphiboles are calcic, rich in iron and Fe-Mg-Mn amphiboles, and range from ferro-hornblende to tschermakite, and tschermakite hornblende. According to various geobarometry methods using the amphibole composition, it is estimated that the calc-alkaline batholith has been formed in a supra-subduction tectonomagmatic environment at 700–900 °C and 0.8–1.5 kbar pressure under high oxygen fugacity. Moreover, based on the thermometry results of feldspars, the emplacement temperature was obtained in the 770–920 °C range by the Anderson method for the Shirkuh granitoid batholith.

Keywords: Shirkuh granitoid; Mineral chemistry; Geobarometry; Supra-subduction; oxygen fugacity.

[1]Ph.D. Student, Department of Petrology, North Tehran Branch, Islamic Azad University, Tehran, Iran. ripsy_567@yahoo.com ORCID: http://orcid.org/0000-0003-3772-2974

[2]Assistant Professor, Department of Geology, North Tehran Branch, Islamic Azad University, Tehran, Iran. *Corresponding author. afshinashjaardalan@yahoo.com ORCID: http://orcid.org/0000-0002-1800-9594

[3]Assistant Professor, Department of Geology, Science and Research Branch, Islamic Azad University, Tehran, Iran. J.sheikhzakaria@gmail.com ORCID: http://orcid.org/0000-0002-4288-572X

[4]Assistant Professor, Department of Geology, Islamshahr Branch, Islamic Azad University, Islamshahr, Iran. ansari@iiau.ac.ir ORCID: http://orcid.org/0000-0001-7539-1892

Revista Geoaraguaia
ISSN:2236-9716
Barra do Garças – MT
v.10, n. esp. Geologia e
Pedologia p.06-32. Dez-2020

RESUMO

O batólito de Shirkuh, Yazd, faz parte da zona estrutural central do Irã, localizada a sudoeste da província. A litologia deste complexo compreende principalmente monzogranito e granodiorito e alguns monzonitos de quartzo, monzodioritos de quartzo e sienogranitos. Plagioclásio, quartzo, ortoclase, biotita e anfibólio são os minerais dominantes nessas rochas. A composição das plagioclases varia de labradorita a oligoclase e os feldspatos alcalinos pertencem à categoria ortoclase. Os anfibólios são cálcicos, ricos em ferro e anfibólios Fe-Mg-Mn, e variam de ferro-hornblenda a tschermakite e tschermakite hornblende. De acordo com vários métodos de geobarometria usando a composição de anfibólio, estima-se que o batólito calcalcalino tenha sido formado em um ambiente tectonomagmático de supra-subducção a 700-900 ° C e 0,8-1,5 kbar sob alta fugacidade de oxigênio. Além disso, com base nos resultados da termometria dos feldspatos, a temperatura de colocação foi obtida na faixa de 770–920 ° C pelo método de Anderson para o batólito granitóide Shirkuh.

Palavras-chave: Granitoide Shirkuh; Química mineral; Geobarometria; Supra-subducção; Fugacidade do oxigênio.

INTRODUÇÃO

The Electron Microprobe (EMP) is a major contributor to progress in petrology, as a field of science, and can provide significant help in identifying rock formations and determining the temperature and pressure conditions of intrusive rocks. Geologists, including Anderson (1997), estimate the formation temperature of rocks based on the chemical composition of plagioclases and the tectonomagmatic classification (Leake, 1971), magmatic origin (Droop, 1987), and oxygen fugacity (Helmy *et al*.,2004), emplacement temperature and pressure (Ernest & Liu, 1998; Johnson Rutherford, 1989) of rock masses based on the chemical composition of amphibole minerals. In this study, the tectonomagmatic classification, magmatic origin and oxygen fugacity are investigated using the chemical composition of feldspars and amphiboles to estimate the geothermobarometry conditions.

RESEARCH METHOD

Revista Geoaraguaia
ISSN:2236-9716
Barra do Garças – MT
v.10, n. esp. Geologia e
Pedologia p.06-32. Dez-2020

Following field investigation, sampling from various lithological units of the rock mass, and detailed petrographic studies, a total of 12 undisturbed samples of the granitoid batholith of Shirkuh were selected for electron microprobe studies in Kansaran Binaloud Co. to determine the chemical composition of amphibole and feldspar minerals. In these samples, 120 points in the feldspar minerals and 30 points in the amphibole minerals were analyzed using an XGT-7200 HORIBA microprobe at a 12 kV accelerating voltage, 15 nA current, 40 s exposure, and exact point analysis at a 10 or 100 µm resolution over an arbitrary point from Na to U (Tables 1 and 2). The results were analyzed and interpreted with the help of Min-Pet and Excel. The chemical formula of amphibole was calculated based on 23 oxygen atoms with an average of 13 and 15 cations, and that of plagioclase based on eight oxygen atoms and five cations.

Quartz monzodiorite

Sample	SiO_2	TiO_2	Al_2O_3	Fe_2O_3	MnO	CaO	Na_2O	K_2O	Cr_2O_3	$An\%$
100-1	61.58	0.1	20.64	0.52	-	10.97	5.35	0.7	-	50.9
100-2	60.8	0.14	21.45	0.42	-	11.11	5.43	0.58	-	51.4
100-4	61.75	-	21.02	0.43	-	10.17	5.82	0.75	-	47.1
100-5	59.88	-	21.72	0.37	-	12.05	5.35	0.56	-	53.8
100-8	60.8	-	20.29	0.43	-	9.98	7.9	0.47	0.08	40.2
100-9	59.8	-	22.93	0.89	-	14.6	0.01	0.82	0.89	93.6
100-10	62.14	-	20.96	0.52	-	9.68	6.19	0.45	0.02	45.2
100-11	63.46	-	21.11	0.58	-	11.25	3.08	0.44	0.04	64.8
100-14	61.55	-	22.24	1.11	-	12.19	1.54	0.9	0.47	76
100-18	59.05	-	22.11	0.49	-	11.83	5.32	1.08	-	52
100-19	59.15	-	21.86	0.38	-	9.68	8.39	0.49	-	38

Quartz monzodiorite

Sample	SiO_2	TiO_2	Al_2O_3	Fe_2O_3	MnO	CaO	Na_2O	K_2O	Cr_2O_3	$An\%$
13-6	57.29	0.78	22.43	0.21	-	11.27	6.35	1.61	-	45.7
13-7	58.45	0.85	20.25	0.25	-	12.11	5.75	2.25	-	48.1
13-8	58.64	-	22.37	0.41	-	12.65	4.75	1.14	-	55.9
13-9	57.68	-	21.84	0.39	-	13.54	6	0.49	-	54.2
13-10	62.15	-	19.37	0.37	-	13.04	4.62	0.39	-	59.6
13-12	56.41	-	18.96	1.35	-	11.8	0.53	10.88	-	45.9
13-13	55.63	-	23.53	0.76	-	17.46	1.52	1.04	-	81.4

13-14	60.1	-	21.79	0.53	-	12.9	3.9	0.72	-	62
13-19	60.42	-	20.38	0.56	-	13.02	4.57	1	-	57.9
13-20	57.96	-	22.61	0.48	-	15.04	3.12	0.74	-	69.7
13-21	87.54	-	6.17	0.17	-	3.88	1.76	0.45	-	51

Syenogranite

Sample	SiO_2	TiO_2	Al_2O_3	Fe_2O_3	MnO	CaO	Na_2O	K_2O	Cr_2O_3	$An\%$
98-1	60.64	-	20.4	0.5	-	11.06	6.45	0.71	0.17	46.9
98-2	63.15	-	19.66	0.5	-	11.58	3.91	1.07	0.06	58.1
98-3	61.87	0.08	20.92	0.48	-	11.87	3.56	0.84	-	61.5
98-4	63.12	0.08	19.96	0.39	-	10.68	4.93	0.52	-	52.8
98-5	96.75	0.57	0.73	0.08	-	0.18	1.43	0.21	-	5.8
98-6	73.83	-	15.62	0.29	-	4.53	5.14	0.49	0.1	31.4
98-7	73.65	-	13.55	0.29	-	4.16	7.81	0.47	0.06	22.1
98-8	64.73	-	18.35	0.34	-	6.44	8.92	1.09	0.08	27
98-9	79.61	-	8.03	0.06	-	1.22	3.97	7.01	0.05	7.3
98-10	69.32	-	18.48	0.24	-	6.34	4.52	1.08	-	40
98-11	71.49	-	16.79	0.21	-	4.28	5.28	1.92	-	26.5
98-12	68.11	-	16.45	0.34	-	6.71	7.14	0.98	-	32.3
98-13	66.27	-	17.84	0.3	-	5.92	8.17	0.82	-	26.1

Granodiorite

Sample	SiO_2	TiO_2	Al_2O_3	Fe_2O_3	MnO	CaO	Na_2O	K_2O	Cr_2O_3	$An\%$
69-1	62.26	-	21.59	0.24	-	9.86	4.07	1.91	-	50.6
69-2	62.3	-	20.33	0.15	-	7.2	8.63	1.34	-	29.5
69-3	64.1	-	18.14	0.16	0.09	6.29	10.04	0.71	-	24.9
69-4	64.83	-	18.91	0.14	0.08	6.84	8.13	0.62	-	30.7
69-5	65.51	-	20.02	0.2	0.01	7.35	5.25	1.21	-	39.1
69-6	63.19	-	21.6	0.26	0.01	8.17	4.39	2.29	-	43.4
69-7	68.51	-	18.56	0.09	-	3.76	8.37	0.65	-	19.1
69-8	63.96	-	22.35	0.21	-	6.74	3.95	2.74	-	39.3
69-9	66.8	-	18.52	0.23	-	5.35	7.42	0.83	-	27
69-10	66.76	-	19.28	0.17	-	6.01	6.97	0.13	-	30.9

Quarts monzonite

Sample	SiO_2	TiO_2	Al_2O_3	Fe_2O_3	MnO	CaO	Na_2O	K_2O	Cr_2O_3	$An\%$
37-1	59.52	-	22.98	0.47	-	11	3.77	2.19	-	53.8
37-2	58.06	-	23.84	0.87	-	11.9	4.1	1.88	-	53.7
37-3	60.24	-	22.58	0.35	-	9.98	3.29	3.51	-	49.6
37-4	60.59	-	22.36	0.25	-	11.89	3.6	1.26	-	59.7
37-5	61.57	-	21.18	0.36	-	9.13	4.46	3.25	-	43.3
37-6	59.03	-	22.05	0.24	-	13.16	4.76	0.7	-	58.2
37-7	59.03	-	22.05	0.24	-	13.16	4.76	0.7	-	58.2

Monzogranite

Sample	SiO_2	TiO_2	Al_2O_3	Fe_2O_3	MnO	CaO	Na_2O	K_2O	Cr_2O_3	$An\%$
88-1	62.46	-	20.33	0.52	-	11.36	4.47	0.79	-	55.7
88-2	60.27	-	20.13	0.37	-	9.5	8.74	0.94	-	35.9
88-3	64.02	-	20.89	0.44	-	11.13	2.34	1.11	-	66.7
88-10	61.17	-	20.79	0.39	-	9.8	7.36	0.5	-	41.3
88-11	62.58	-	20.33	0.45	-	10.43	5.26	0.73	-	50.1
Monzogranite										
Sample	SiO_2	TiO_2	Al_2O_3	Fe_2O_3	MnO	CaO	Na_2O	K_2O	Cr_2O_3	$An\%$
44-1	56.97	-	23.19	0.19	0.04	12.73	6.23	0.59	-	51.5
44-2	58.18	-	22.1	0.24	0.03	14.35	4.39	0.64	-	62.2
44-3	61.23	-	21.77	0.19	0.03	12.56	3.59	0.48	-	64.1
44-4	89.21	-	6.39	0.11	0.15	2.66	1.26	0.18	-	51.6
44-5	59.07	-	21.35	0.11	-	11.73	7.21	0.49	-	46.2
44-6	59.01	-	22.58	0.11	-	14.14	3.66	0.43	-	66.5
44-7	59.5	-	21.85	0.14	-	12.35	5.53	0.57	-	53.6
44-8	60.94	-	21.47	0.18	-	13.01	3.61	0.75	-	63.7
44-9	60.92	-	22.88	0.19	-	13.06	2.33	0.57	-	72.7
44-10	60.03	-	23.52	0.2	-	12.41	3.25	0.54	-	65.5
44-11	59.21	-	21.09	0.21	-	12.1	6.83	0.51	-	48.3
44-12	55.75	-	22.09	0.2	0.07	12.77	8.26	0.8	-	44.5
44-13	58.64	-	22.74	0.19	0.16	12.73	4.51	0.98	-	57.7
44-14	58.77	-	21.36	0.25	0.13	10.48	6.04	2.92	-	42.1
44-15	60.25	-	22.37	0.18	0.19	10.64	4.44	1.88	-	50.9
Monzogranite										
Sample	SiO_2	TiO_2	Al_2O_3	Fe_2O_3	MnO	CaO	Na_2O	K_2O	Cr_2O_3	$An\%$
46-1	56.83	-	22.57	0.19	-	13.53	6	0.81	-	53.4
46-2	60.48	-	21.76	0.13	-	13	4.04	0.52	-	62.1
46-3	58.34	-	21.36	0.15	-	13.44	6.2	0.42	-	53.4
46-4	59.1	-	22.96	0.15	-	13.53	2.94	0.69	-	68.8
46-5	56.32	-	20.28	0.14	-	12.79	9.29	0.52	-	42.3
46-6	57.69	-	22.44	0.16	-	13.48	5.38	0.5	-	56.6
46-7	58.58	-	21.47	0.08	-	12.41	7.18	0.27	-	48.2
46-8	59.23	-	21.76	0.16	-	13.04	5.31	0.44	-	56.3
46-9	57.62	-	21.75	0.13	-	13.6	6.59	0.32	-	52.5
46-10	56.32	-	22.13	0.26	-	12.05	8.97	0.23	-	42.2
46-11	56.66	-	23.18	0.19	-	13.31	6.38	0.24	-	52.9
46-12	61.59	-	22.76	0.26	-	15	-	0.34	-	97.4
46-14	59.04	0.56	22.3	0.12	0.03	12.09	5.31	0.5	-	54.2
46-15	58.86	0.52	21.32	0.1	0.03	11.24	7.6	0.3	-	44.3
46-16	58.87	0.62	20.22	0.12	0.03	11.57	7.028	0.54	-	45.6
Monzogranite										

Sample	SiO_2	TiO_2	Al_2O_3	Fe_2O_3	MnO	CaO	Na_2O	K_2O	Cr_2O_3	$An\%$
82-1	60.22	-	22.9	0.21	-	14.13	1.82	0.65	-	77.6
82-2	59.53	-	21.63	0.19	-	12.76	5.2	0.63	-	55.7
82-5	59.28	-	21.21	0.39	-	14.43	3.16	1.46	-	65.9
82-6	58.71	-	21.71	0.16	-	12.85	6.09	0.42	-	52.7
82-7	87.85	-	4.72	0.23	-	1	1.21	4.95	-	11
82-8	69.35	-	12.06	0.07	-	0.38	2.07	16.01	-	1.6
82-9	61.52	-	21.06	0.21	-	10.97	4.07	2.12	-	52.6
82-10	57.01	-	21.79	0.16	-	14.82	5.7	0.47	-	57.7
82-11	56.93	-	23.35	0.15	-	12.99	6.16	0.42	-	52.7
82-12	60.39	-	22.24	0.18	-	13.39	3.3	0.51	-	67.1
82-13	59.98	-	22.67	0.07	-	12.83	3.89	0.56	-	62.5
Monzogranite										
Sample	SiO_2	TiO_2	Al_2O_3	Fe_2O_3	MnO	CaO	Na_2O	K_2O	Cr_2O_3	$An\%$
81-1	72.22	-	18.47	0.06	0.01	3.71	4.79	0.72	-	28
81-2	72.22	-	18.47	0.06	0.01	3.71	4.79	0.72	-	28
81-3	67.37	-	18.15	0.05	-	4.18	9.33	0.92	-	18.9
81-4	66.96	-	18.79	0.03	-	4.88	8.49	0.85	-	22.9
Monzogranite										
Sample	SiO_2	TiO_2	Al_2O_3	Fe_2O_3	MnO	CaO	Na_2O	K_2O	Cr_2O_3	$An\%$
95-1	60.35	-	21.46	0.54	-	11.97	3.91	1.24	-	58.3
95-2	49.85	-	25.06	0.97	-	18.76	4.37	0.43	-	69
95-5	61.82	-	21.4	0.7	0.12	10.36	4.51	1.04	-	52.4
95-6	63.8	-	19.62	0.45	0.11	10.05	4.12	1.8	-	51.1
95-9	61.77	-	19.74	0.72	-	9.58	6.97	1.21	0.01	40.5
95-10	60.76	-	20.34	0.43	-	11.62	6.16	0.54	0.15	49.6
95-13	63.56	-	22.31	0.73	-	10.37	1.9	0.98	0.1	69.3
95-14	64.1	-	21.62	0.47	-	11.2	1.47	1.05	0.04	74.1
Monzogranite										
Sample	SiO_2	TiO_2	Al_2O_3	Fe_2O_3	MnO	CaO	Na_2O	K_2O	Cr_2O_3	$An\%$
35-6	59.74	-	20.69	0.13	-	12.38	6.17	0.83	-	50.5
35-7	59.34	-	21.33	0.18	-	12.52	5.49	1.09	-	52.7
35-8	59.09	-	21.86	0.13	-	11.49	6.32	1.07	-	47.5
35-9	59.34	-	21.33	0.18	-	12.52	5.49	1.09	-	52.7
35-10	59.34	-	21.33	0.18	-	12.52	5.49	1.09	-	52.7
35-11	59.02	-	22.07	0.14	0.26	13.95	3.94	0.56	-	64.1
35-12	56.89	-	23.01	1.2	0.23	12.1	6.19	0.3	-	51.1
35-13	59.53	-	22.03	0.19	0.19	13.2	4.19	0.62	-	61.3

Table 1. The results of electron microprobe analysis for plagioclases collected from Shirkuh, Yazd, Iran. Source: Authors (2020).

Revista Geoaraguaia
ISSN:2236-9716
Barra do Garças – MT
v.10, n. esp. Geologia e
Pedologia p.06-32. Dez-2020

Sample	SiO_2	TiO_2	Al_2O_3	FeO	MnO	MgO	CaO	K_2O	P_2O_5
100-3	39.44	3.48	4.66	21.54	0.64	10.8	13.52	0.83	-
100-6	41.75	2.42	4.69	23.03	0.83	8.57	13.55	0.98	-
100-7	40.86	2.02	4.75	23.81	0.65	9.65	13.77	0.86	-
100-12	38.82	3.02	4.48	21.52	0.78	10.63	13.88	0.84	0.83
100-13	42.1	1.34	3.52	22.43	0.99	10.01	14.69	0.55	1.01
100-16	37.21	12.99	3.34	4.35	0.63	7.58	18.56	0.36	-
100-17	42.32	3.34	4.95	20.25	0.66	8.96	13.36	1.02	-
95-3	38.58	2.49	6.17	23.79	0.99	9.27	13.4	0.85	-
95-4	40.84	1.33	3.88	25.25	1.44	10.71	12.72	0.62	-
95-7	37.34	3.21	5.71	26.98	1.37	8.38	9.47	2.75	-
95-8	40.51	2.17	4.28	25.72	1.27	9.37	11.08	1.84	-
95-11	41.45	2.51	5.4	22.04	0.75	9.09	12.82	1.36	-
95-12	41.39	2.13	5.43	23.04	0.9	9.36	12.69	0.79	-
95-15	40.72	2.43	5.71	21.16	0.88	9.68	13.85	1.16	0.17
95-16	41.24	2.17	5.03	20.01	0.82	9.67	14.77	1.04	1.18
88-4	40.4	2.14	4.91	22.8	0.77	10.31	14.04	0.8	-
88-5	43.66	1.91	6.52	20.71	0.84	8.52	13.48	0.69	-
88-6	41.77	1.77	4.33	23.79	1.14	10.4	13.12	0.5	-
88-7	41.88	1.44	3.99	25.04	1.36	9.32	13.39	0.51	-
88-8	39.46	1.74	4.36	25.53	1.15	9.18	13.86	0.82	0.5
88-9	39.46	1.74	4.36	25.53	1.15	9.18	13.86	0.82	0.5
88-12	37.84	2.21	4.31	21.98	0.75	10.06	15.62	0.78	2.63
88-13	38.86	1.95	5.03	22.94	0.74	10.82	14.09	0.79	1.11
88-14	38.55	1.75	5.39	28.16	1.02	9.94	11.29	0.51	0.01
88-15	41.33	1.91	4.39	24.01	1	9.89	13.19	0.61	0.06
88-16	40.14	1.98	4.35	24.66	1.05	9.72	13.68	0.71	-
88-17	40.65	1.67	4.49	25.25	1.22	8.94	13.6	0.68	-
13-5	42.73	0.91	4.51	26.27	0.97	7.33	13.88	0.88	-
13-22	46.14	0.72	3.95	25.62	1.03	8.04	11.38	0.78	-
13-23	41.25	1.48	5.14	26.2	1.06	6.84	13.06	1.89	-

Table 2. The results of electron microprobe analysis for amphiboles collected from Shirkuh, Yazd, Iran. Source: Authors (2020).

Revista Geoaraguaia
ISSN:2236-9716
Barra do Garças – MT
v.10, n. esp. Geologia e
Pedologia p.06-32. Dez-2020

GEOLOGY OF THE REGION

With a 1000 km2 outcrop, the granitoid batholith of Shirkuh is located in the coordinates range 31° 23’ to 31° 45’ N and 53° 50’ to 20° 54’ E, in Yazd Province, southeast of Taft and west of Mehriz, Iran (Figure 1).

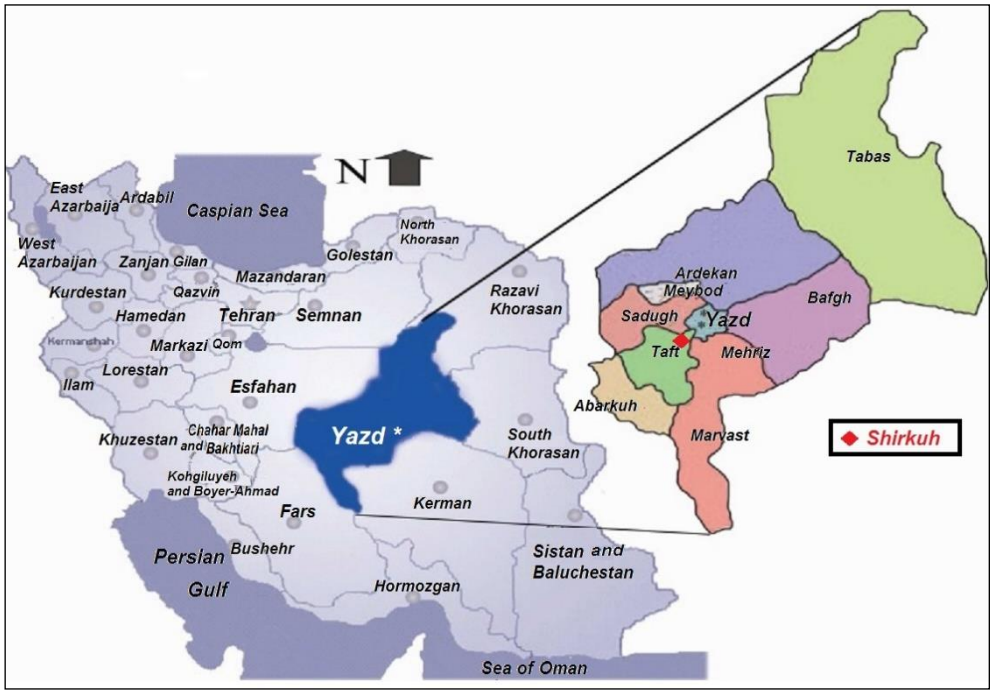

Figure 1. Geography of Yazd Province on the map of Iran (courtesy of Natural Geography of Yazd Province). Source: Authors (2020).

According to the structural zones of Iran, the study range is situated in Central Iran (Stocklin. 1988) and in the middle of the Urmia–Dokhtar volcanic belt (Figure 2). The geological map of Iran (courtesy of Moine-Vaziri, 1985) dates back this region to the volcanic period of The Paleocene. Shirkuh batholith, having cut through the Nayband formation (Upper Triassic) with Cretaceous limestones and a sandstone and conglomerate unit (Lower Cretaceous) lying on top as an angular unconformity, probably dates back to the Jurassic.

The Shirkuh granite is younger than the Nayband formation but older than those from the Cretaceous. Forster (1972) dated the Shirkuh granite by the Rb–Sr method at

176±10 million years, whereas Rir and Mohafez (1972) dated the Shirkuh granitoid feldspars at 159–186 million years by the K–Ar method.

The said batholith is composed of five rock units, namely monzogranite, granodiorite, quartz monzonite, quartz monzodiorite, and syenogranite. Monzogranites, as the largest unit, form the main body of the batholith.

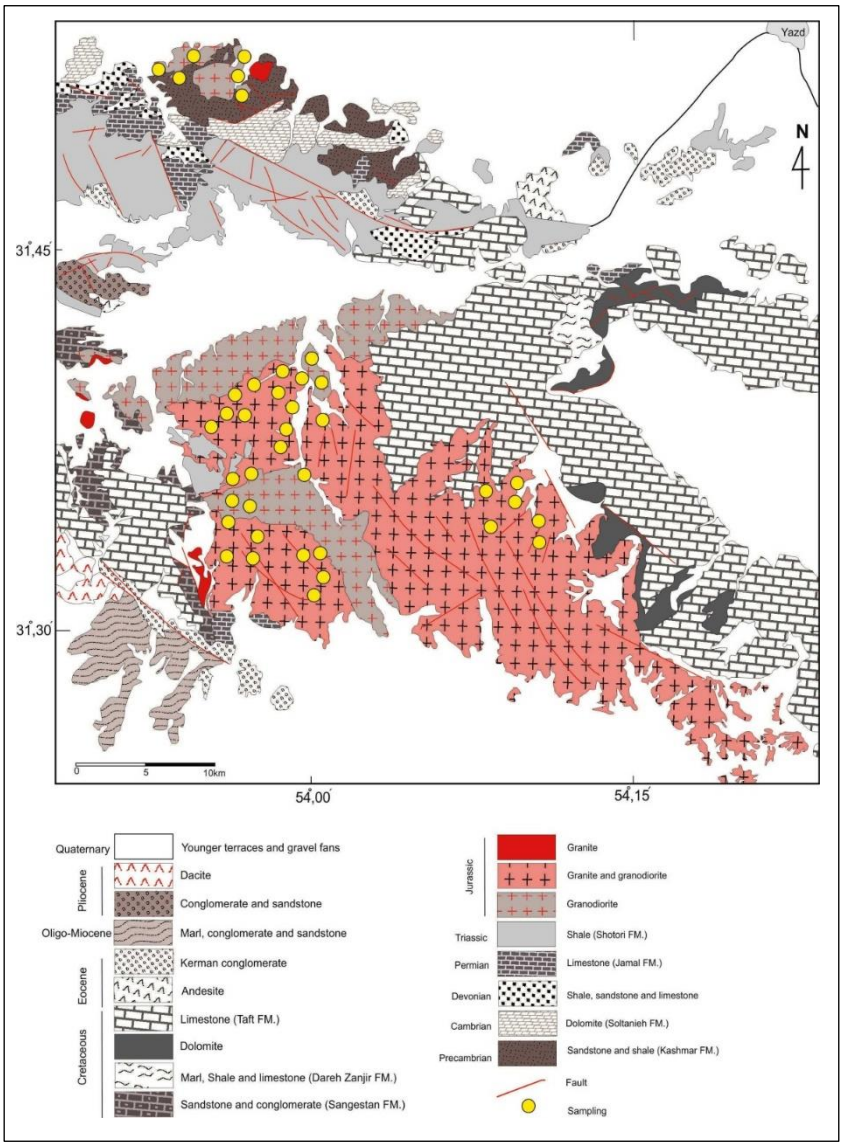

Figure 2. The situation of the study region east of the 1:100000 map of Khezrabad (Hajmolla'ali, 1993), west of the 1:100000 map of Yazd (Hajmolla'ali, 2000), north of the 1:100000 map of Nir (Shahraki Ghadimi, 2008), and north of the 1:100000 map of Dehshir (Sabze'i, 1997).
Source: Authors (2020).

PETROGRAPHY

Based on the petrographic studies and the modal analysis (Figure 3), the batholith complex of Shirkuh is composed of an acidic part consisting of monzogranite, granodiorite, and syenogranite, and an intermediate part consisting of quartz monzonite and quartz monzodiorite. The major minerals include quartz, plagioclase and orthoclase, and the minor minerals are biotite, amphibole, muscovite, garnet, tourmaline, epidote, zircon, sphene and apatite (Az Mikaelians, 2020). It is noteworthy that amphibole is the primary mineral in the monzogranite and quartz monzodiorite units.

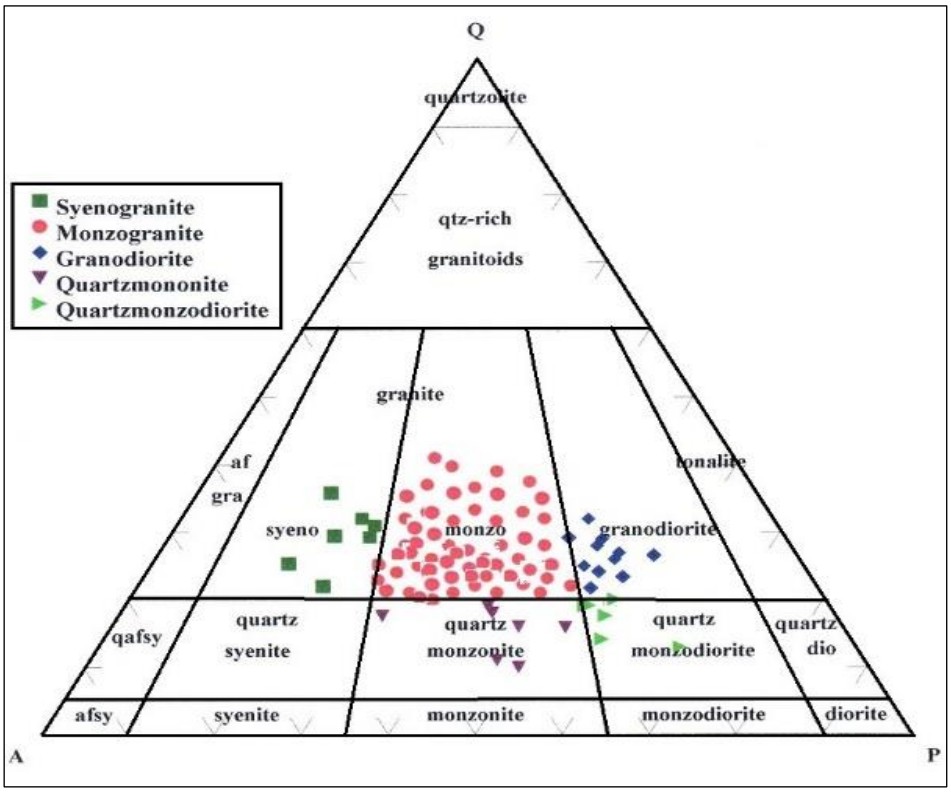

Figure 3. Modal classification of the samples collected from the Shirkuh granitoid batholith (1973). Source: Authors (2020).

MINERAL CHEMISTRY

Twelve cross-sections of the plagioclase and amphibole minerals were analyzed by the electron microprobe to identify the physiochemical conditions of the magma, forming the granitoid batholith of Shirkuh.

FELDSPAR CHEMISTRY (THE COMPOSITION OF FELDSPARS WITH DIFFERENTIATION OF ROCK UNITS)

Some plagioclases in the intrusive masses studied by microscopy showed zoning, whereas others did not show any zoning. Therefore, both types of plagioclases were analyzed by the electron microprobe. In general, the chemical composition of zoning-free plagioclases varies from labradorite to oligoclase but is mainly concentrated in the labradorite range (Figures 4, 5, 6a, b, c). Nonetheless, the core is richer in sodium than the margin in the zoning plagioclases, indicating reverse zoning. Both regular and reverse zonings are observed in the plagioclases.

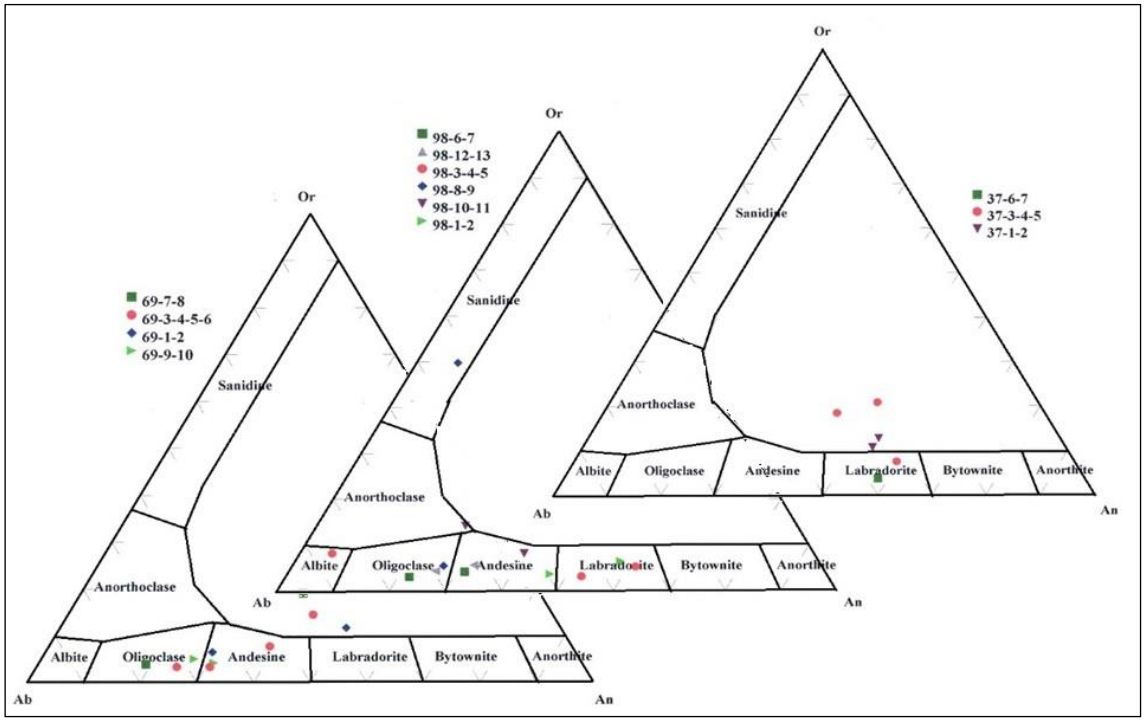

Figure 4. The normative Ab-An-Or ternary diagram for the probed granodiorite [69], syenogranite [98] and Quarts monzonite [37] plagioclases.
Source: Authors (2020).

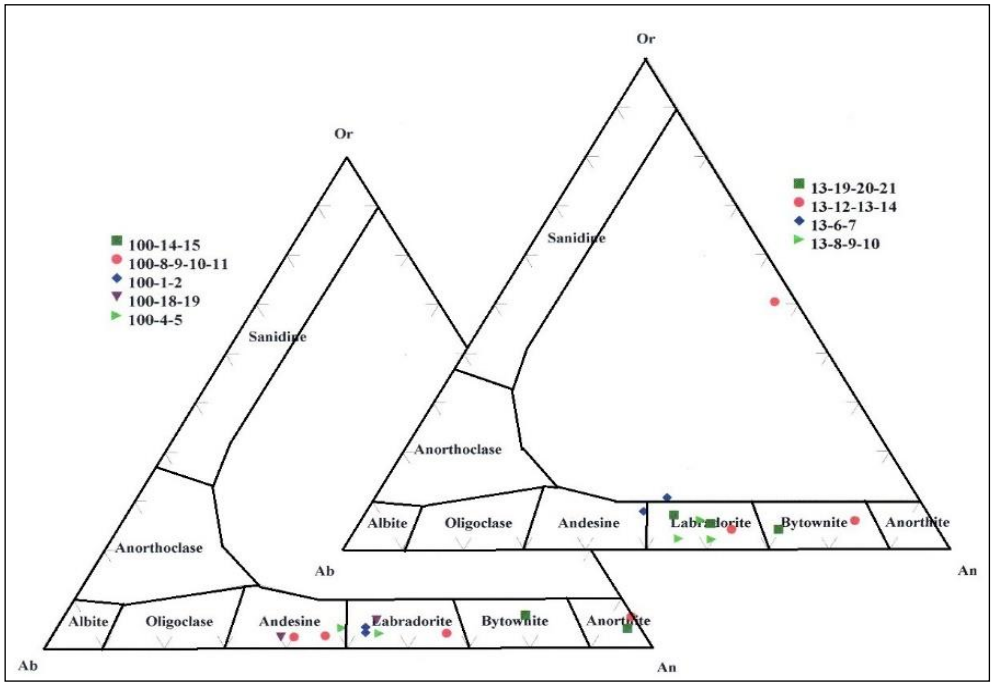

Figure 5. The normative Ab-An-Or ternary diagram for the probed Quartz monzodiorite [13, 100]. Source: Authors (2020).

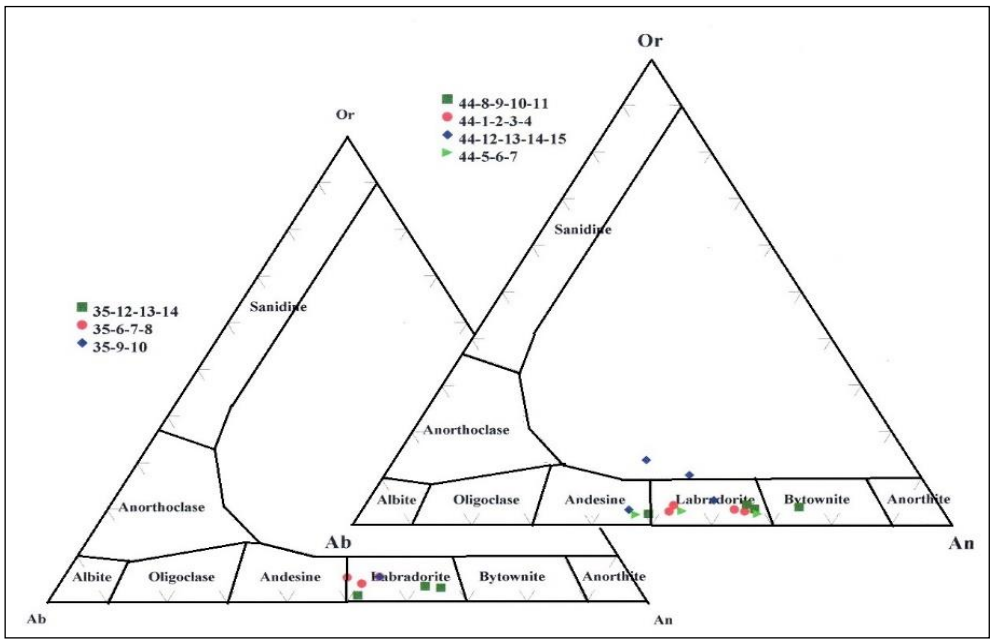

Figure 6a. The normative Ab-An-Or ternary diagram for the probed monzogranite [35, 44]. Source: Authors (2020).

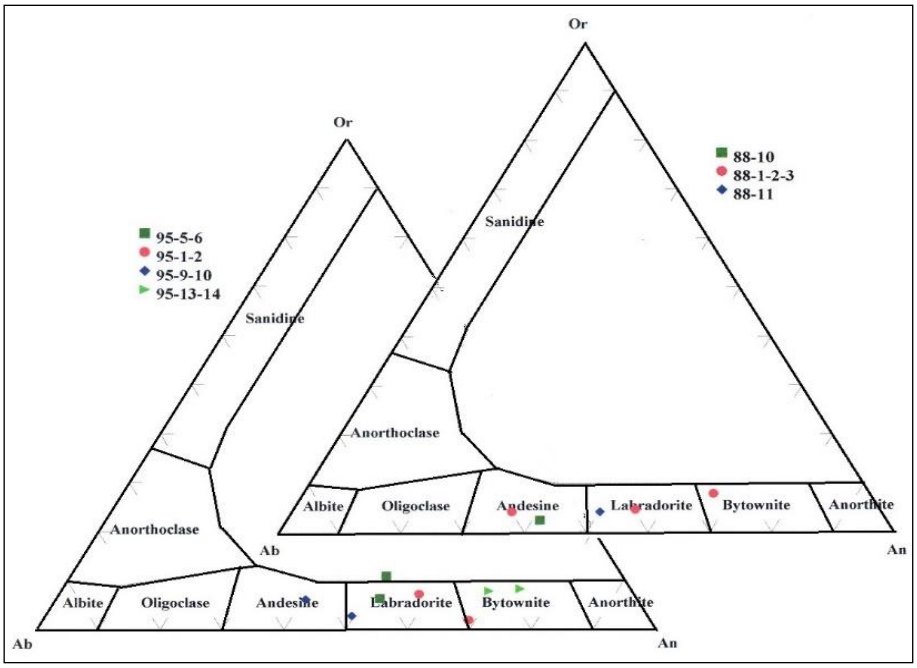

Figure 6b. The normative Ab-An-Or ternary diagram for the probed monzogranite [88,95]. Source: Authors (2020).

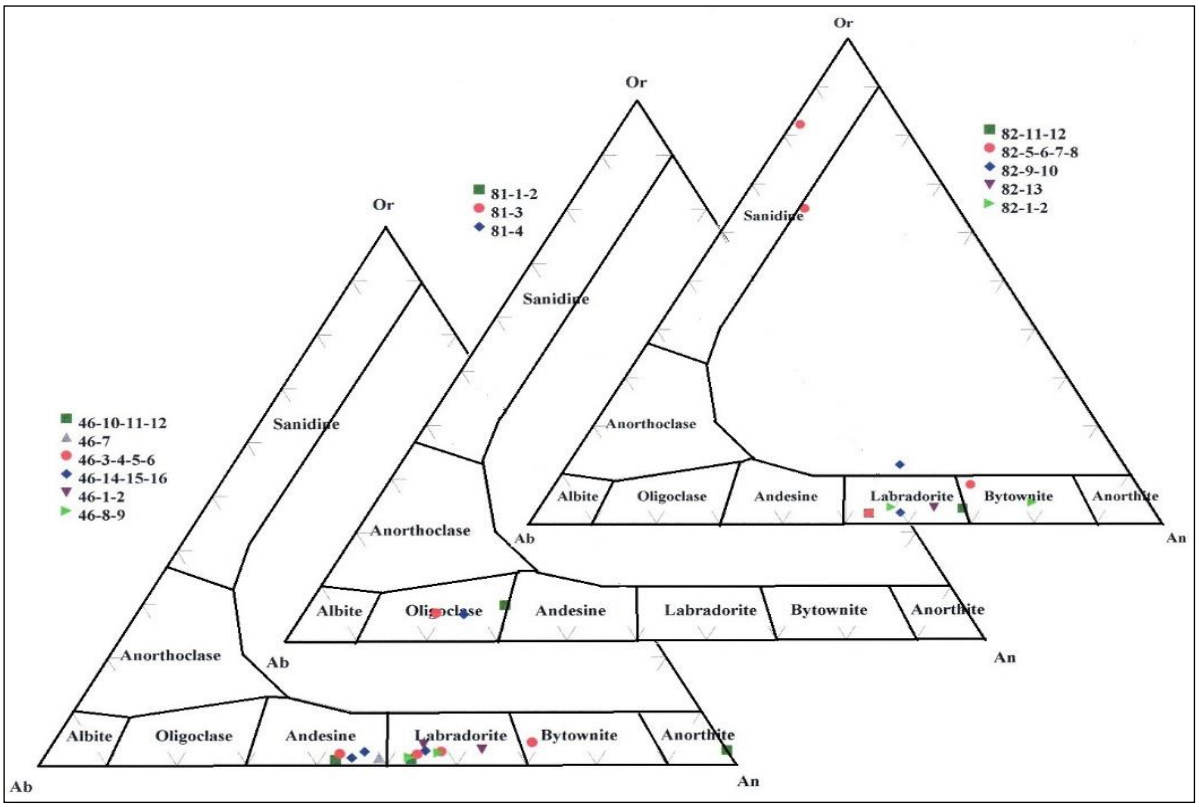

Figure 6c. The normative Ab-An-Or ternary diagram for the probed monzogranite [82,81,46] Source: Authors (2020).

THERMOMETRY OF FELDSPARS

The results obtained from the analysis of feldspars are matched on the normative Ab-An-Or ternary diagram (Anderson, 1996) (Figure 7). Based on this method, a temperature ranges of 770 to 920 °C was determined for the granitoid rocks of Shirkuh (assuming a 1 kbar pressure).

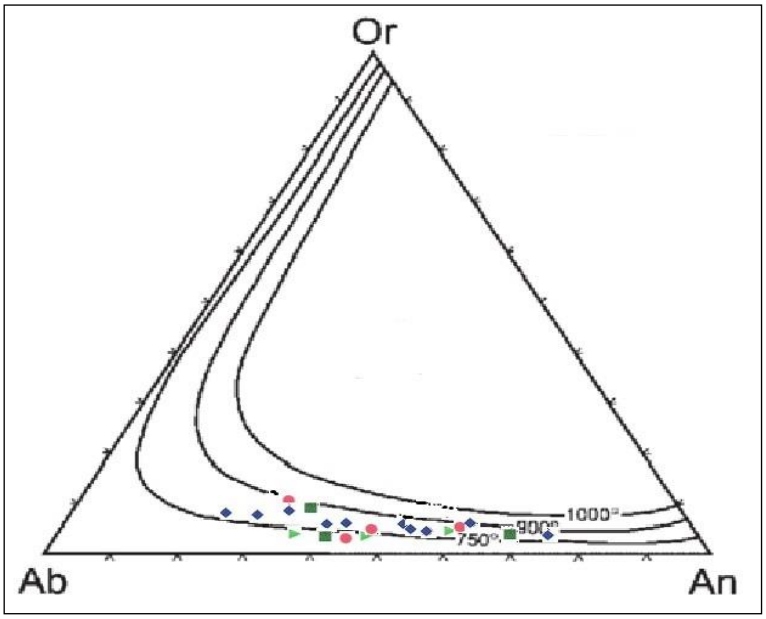

Figure 7. The Ab-An-Or thermometry diagram for determining the equilibrium temperature of feldspar minerals in the probed samples at a pressure of 1 kbar.
Source: Anderson (1996); Carle (1993).

AMPHIBOLE CHEMISTRY

According to Leake *et al.* (1997) zoning, the amphiboles in the Shirkuh batholithic complex are placed into two main categories of Fe-Mg-Mn and calcic amphiboles (Figure 8a). The composition of amphiboles is of tschermakite (at high pressures, anorthite diffuses into the hornblende structure and converts it into tschermakite (Best, 2003), hornblende, and tschermakite hornblende types (Figure 8b).

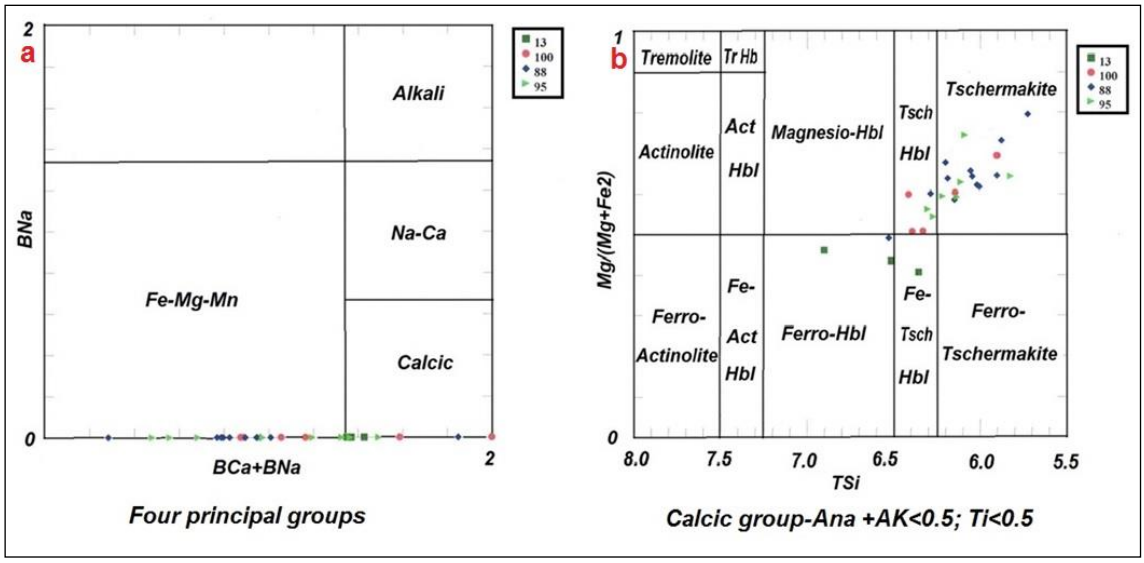

Figure 8. (a) Classification of amphiboles based on the average of 13 and 15 cations (Avg15-NK, 13-CNK) and *(b)* nomenclature of amphiboles based on their composition.
Source: Leake *et al*. (1997).

Since the Fe3+ level in the structural formula of amphiboles in quartz monzodiorite and monzogranite is greater than 1 (the structural formula of amphiboles was calculated based on the average of 13 and 15 cations (Avg15-NK,13-CNK)), the prefix "ferro" can be used for naming the hornblendes in these rocks. The amphiboles collected from the study area lack Na.

TECTONOMAGMATIC CLASSIFICATION OF AMPHIBOLES

The geochemical forms of amphiboles, consisting primarily of mantle xenoliths, were evaluated to identify metasomatism features in intraplate and supra-subduction tectonomagmatic environments. The amphiboles formed in the mantle wedge above the subduction zone (S-Amph) contain lower TiO2 and Na2O levels than intraplate amphiboles (I-Amph) (Coltori et al.,2007). However, these two groups considerably overlap. Based on the tectonomagmatic diagram of Na2O versus SiO2, the amphiboles in the Shirkuh granitoid batholith are of S-Amph type depending on the subduction environment (Figure 9).

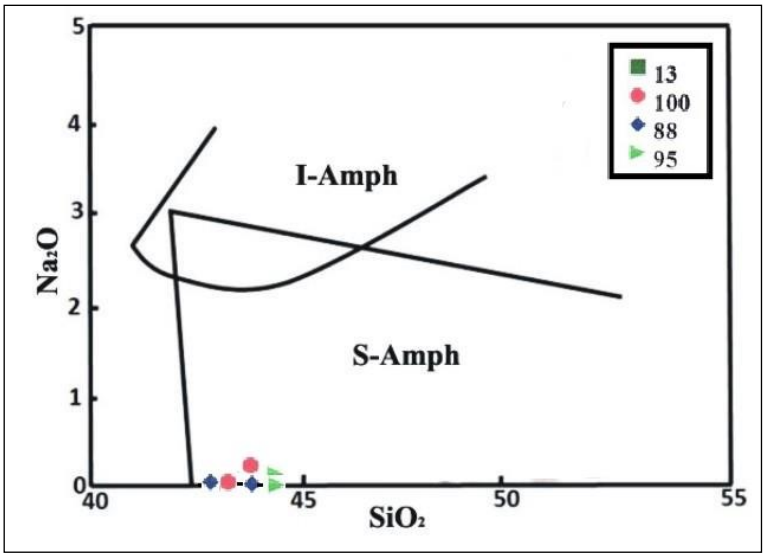

Figure 9. Determination of the tectonic environment of amphiboles.
Source: Coltori *et al*.(2007).

The presence of amphibole crystals may raise the question of whether local amphiboles are magmatic or metamorphic? The significance of this issue is further highlighted in the geothermometry and geobarometry of amphiboles for determining the crystallization conditions of the granitoid mass. Based on the Si variations versus Na+Ca+K (Leake et al., 1997), all points analyzed in the amphiboles are placed within the range of magmatic (igneous) amphiboles (Figure 10a, b).

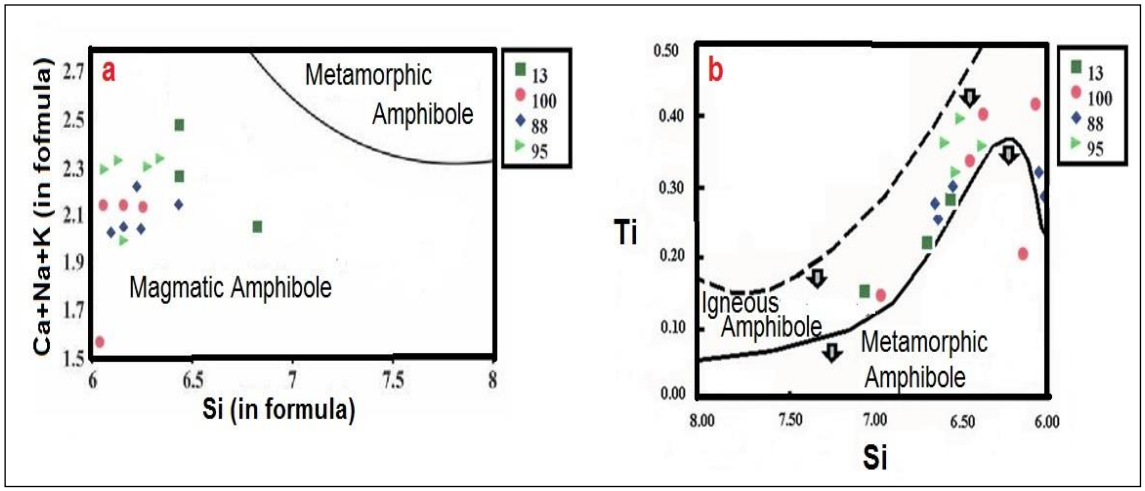

Figure 10. (a) The composition of amphibole crystals in the Shirkuh intrusive mass, all points are in the range of igneous amphiboles and *(b)* differentiation of metamorphic and magmatic amphiboles.
Soirce: Leake *et al*. (1997).

MAGMATIC ORIGIN

The composition of amphiboles can be used to determine the genesis and tectonomagmatic environment of igneous rocks. Most scholars believe that the presence of calcic amphiboles in the granitoid rocks indicates that the rocks are Type I granitoids due to their high CaO levels, which eventually leads to the crystallization of hornblendes (Chappel and White, 1974; White and Chappel, 1983; Whborn *et al.*,1981; Clemens and Wall,1984; Stein and Dietl, 2001).

The diagram designed by Droop (1987) allows differentiation of calc-alkaline, alkaline, ultramafic, and lamprophyric amphiboles based on the SiO_2 and TiO_2 levels (Figure 11).

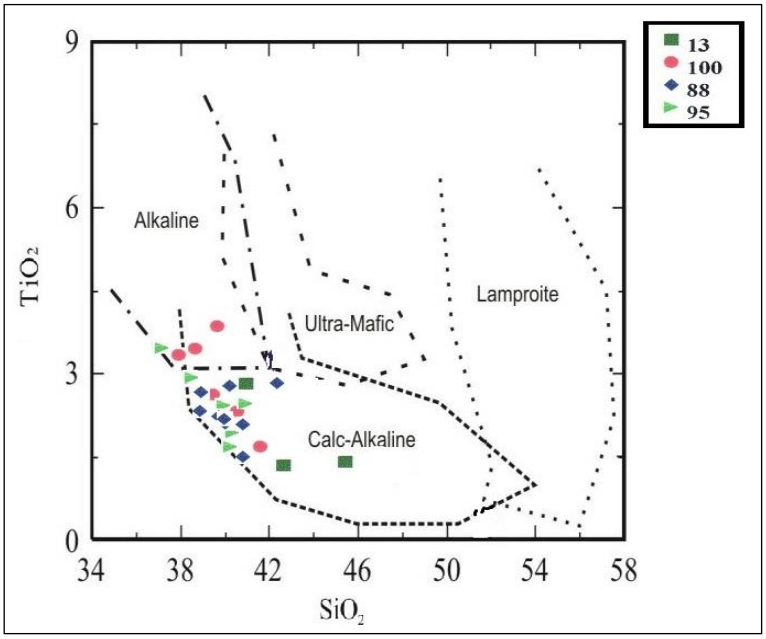

Figure 11. Differentiation of the tectonic environment of the Shirkuh batholitic intrusive complex by the chemical composition of amphiboles.
Source: Droop (1987).

Plotting the studied amphiboles on this diagram reveals that most samples fall in the calc-alkaline range and some in the alkaline range. On the other hand, $Mg^{\#}$ (magnesium number) in hornblendes is a crucial factor for identifying their magmatic origin (Xie and Zhang,1990; Huaimin et al.,2006). $Mg^{\#}$ levels of higher than 0.7 and less than 0.5 show the

Revista Geoaraguaia
ISSN:2236-9716
Barra do Garças – MT
v.10, n. esp. Geologia e
Pedologia p.06-32. Dez-2020

mantle and crustal origin, whereas an $Mg^{\#}$ level of 0.5–0.7 is suggestive of a combined mantle-crustal origin. Table 2 shows the $Mg^{\#}$ level in the monzogranite and quartz monzodiorite amphiboles. As seen, all rocks have a mantle origin (Table 3).

Hornblende Sample No.	$Mg^{\#}$ level	Origin
13 – 22	0/79	Mantle
13 - 5	0/79	Mantle
13 - 23	0.84	Mantle
88 - 5	0.83	Mantle
88 - 7	0.8	Mantle
95 - 11	0.77	Mantle
95 - 16	0.91	Mantle
100 - 17	0.78	Mantle
100 - 6	0.87	Mantle
100 - 13	0.86	Mantle

Table 3. The origin of amphiboles
Source: Authors (2020).

DETERMINATION OF OXYGEN FUGACITY FROM AMPHIBOLE COMPOSITION

The oxygen fugacity is among the factors affecting the minerals in a rock. The chemical composition of amphiboles containing Al^{IV}>0.75 and Fe^{Total}/ Fe^{Total}+Mg>0.3 can be used for determining the oxygen fugacity in the intrusive rocks. All the amphiboles analyzed in this study meet these conditions. The Al^{IV} variations against Fe^{Total}/ Fe^{Total}+Mg indicate that all amphiboles are placed in a wide range with a high oxygen fugacity (Helmy et al.,2004), revealing that Shirkuh granitoids were formed in relation to the boundary of convergent plates (Anderson, Smith, 1995; Anderson, 1997) (Figure 12).

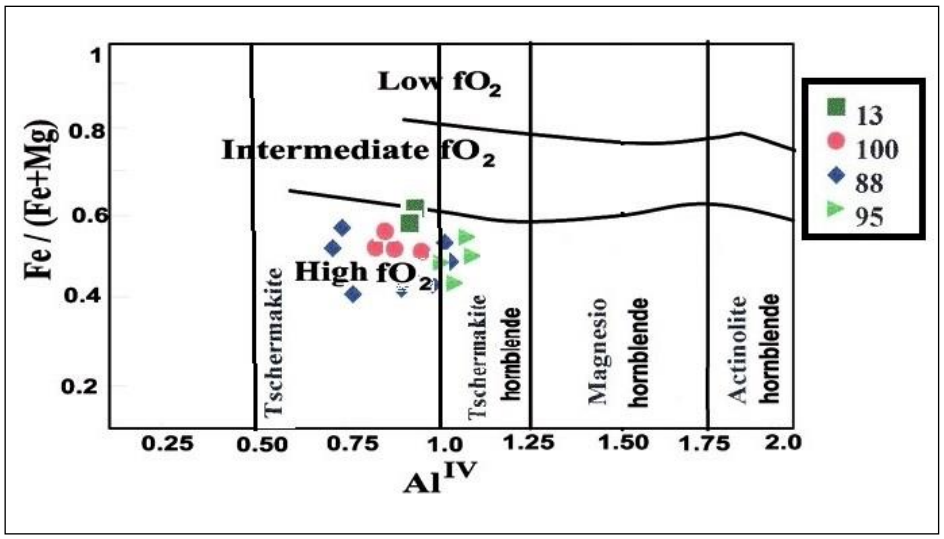

Figure 12. Determination of oxygen fugacity from amphibole composition.
Source: Helmy *et al*. (2004).

THERMOBAROMETRY OF MAFIC ROCKS

The aluminum and titanium levels on the margin of amphibole minerals were used to calculate the geothermometry of the samples. Based on the Ernst and Liu (1998) method, the geothermometry of the amphibole margins indicates a temperature of 650-950 °C for lamprophyric amphiboles (Figure 13).

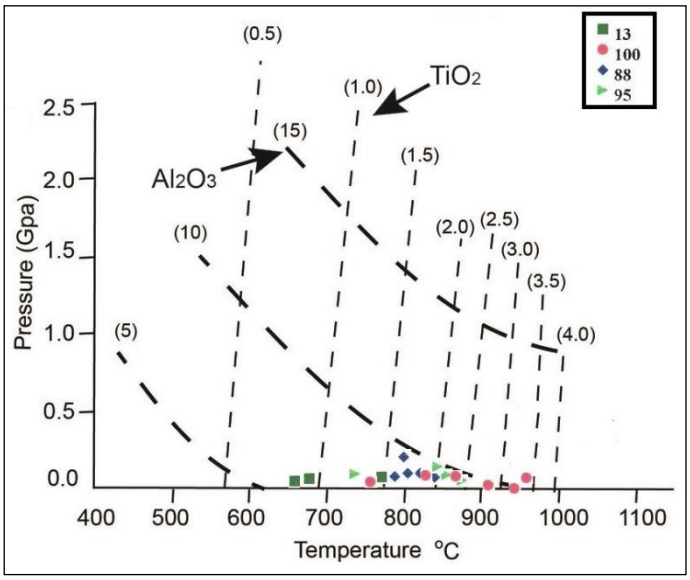

Figure 13. Al_2O_3 and TiO_2 isoplates in amphiboles based on the weight percentage as a function of temperature and pressure
Source: Ernst and Liu (1998).

Revista Geoaraguaia
ISSN:2236-9716
Barra do Garças – MT
v.10, n. esp. Geologia e
Pedologia p.06-32. Dez-2020

Amphiboles are suitable to evaluate the P-T conditions of calc-alkaline intrusive masses. Hornblende often exists in these rocks and is stable in wide pressure and temperature ranges of 1–23 kbar and 400–1150 °C, respectively. The mineral is the most useful in geothermobarometry studies. The hornblende-plagioclase thermometry and aluminum geobarometry of hornblendes are suitable to detect temperatures at which granites are emplaced (Blundy & Holland, 1990; Holland & Blundy, 1994; Stein & Dietl, 2001; Ernst, 2000).

Four conventional tectonic methods were used based on the amphibole Al content to estimate the crystallization pressure of the selected amphiboles. The Al content varies with the emplacement depth of masses and is dependent on the environment and multiple factors leading to an error in the calculated pressure. Table 4 summarizes the calculated crystallization pressure of amphiboles and their chemical formula.

1.P(±3Kbar)= -3.92+5.03Al(total),(Hammarstron & Zen 1986)

2.P(±0.5Kbar)= -3.46+4.23Al(total),(Johnson & Rutherford 1989)

3.P(±0.6Kbar)= -3.01+4.76Al(total),(Sehmidth 1992)

4.P(±1.0Kbar)= -4.76+5.64Al(total),(Hollister & Grissorn 1987)

Sample No.	Al Total	Hammarstron & Zen 1986	Johnson & Rutherford 1989	Sehmidth 1992	Hollister & Grissorn 1987
13-5	0.81	0.1	-0.5	0.8	-0.2
13-22	0.7	-0.4	-0.5	0.3	-0.8
13-23	0.93	0.75	0.3	1.4	0.5
88- 5	1.2	2.1	1.6	2.7	2
88-7	0.7	-0.4	-0.5	0.3	-0.8
95-11	1	1.1	0.77	1.8	0.9
95-16	0.9	0.6	0.3	1.3	0.5
100-6	0.83	0.1	-0.5	0.94	-0.1

100-13	0.63	-0.9	-0.9	-0.01	-1.2
100-17	0.9	0.6	0.3	1.3	0.31

*Table 4***.** The calculated crystallization pressure of amphiboles.
Source: Authors (2020).

In all these four methods, the pressure in the environment is related to the total Al, and other parameters such as temperature are not considered. Given the negligible AlTotal in some quartz monzodiorite and monzodiorite amphiboles of Shirkuh batholith, the resulting negative pressure is suggestive of amphibole crystallization at very low pressure and low depth (Esmaeili *et al*., 2013), which is also confirmed by the Ti level in the amphiboles of the Shirkuh batholitic mass indicating a pressure of below 1 kbar. In comparison with Al, Ti ion has a larger ionic radius and thus is less affected by the pressure rise. However, the Ti level increases in the amphibole with increasing temperature (Moody *et al*., 1983; Ernst, 2002) (Figure 14).

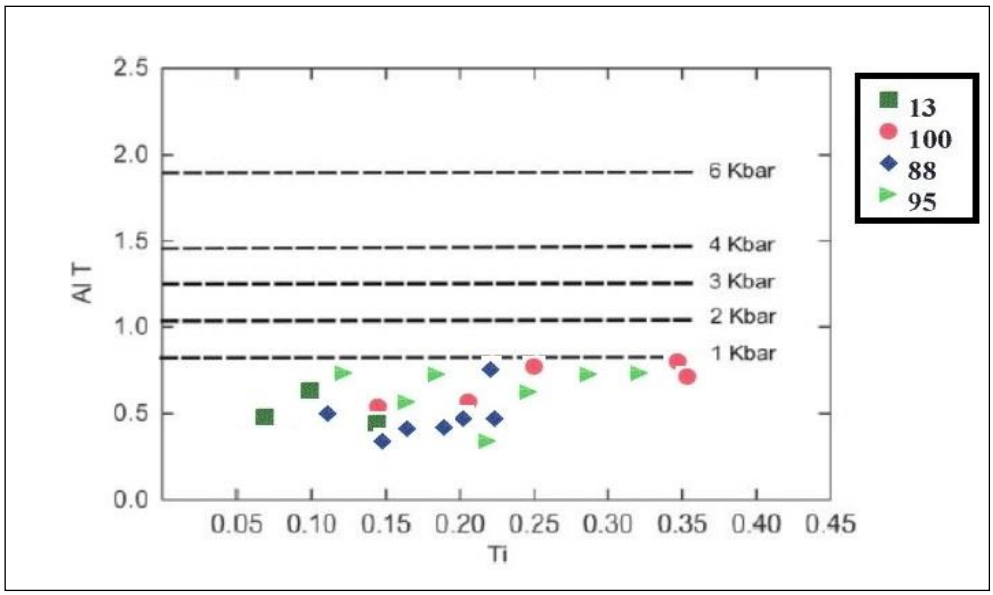

Figure 14: The total Al as a function of Ti level.
Source: Schmidt (1992).

The temperature rises, increasing the Ti level from 0.07 cation in the formula unit at 650 °C to 0.01-0.14 at 700 °C, 0.15-0.22 at 800 °C, 0.23-0.27 at 900 °C and 0.3-0.35 at 950 °C

Revista Geoaraguaia
ISSN:2236-9716
Barra do Garças – MT
v.10, n. esp. Geologia e
Pedologia p.06-32. Dez-2020

(Ernest & Liu, 1998). Based on the Ti level in the hornblendes of quartz monzodiorite (0.081-0.38) and monzogranite (0.123-0.286), a temperature ranges of 675 to 975 °C is estimated, whereas a temperature ranges of 679 to 972 °C is estimated for the formation of amphiboles based on the thermometry conducted by Colombi (1989) (Table 5).

Thermometry T (°C)
Colombi 1989
Ti<0.08, T(°C)= 2816*Ti+445
Ti>0.08, T(°C)= 980*Ti+600

Sample No.	13-5	13-22	13-23	88-5	88-7	95-11	95-16	100-6	100-13	100-17
CTi	0.104	0.081	0.172	0.215	0.163	0.286	0.123	0.276	0.154	0.381
T(˚C)	701	679	768	811	760	880	720	870	751	972

Table 5. The amphibole formation temperature range
Source: Authors (2020).

According to Hollister (1983), the magma temperature for hydrous magmas ranges from 700 to 900 °C, and this temperature is relatively independent of pressure. However, Anderson (1983) found an increase in the Ti level in hornblendes with increasing temperature. Furthermore, Helz (1993) evaluated the formation temperature of amphibole minerals using variations of Al level relative to the Ti level in their formula unit. In this study, an approximate temperature ranges of 720 to 875 °C was obtained using Ti variations versus Al^{Total} for crystallization of hornblendes of those intrusive rocks in the region, preserving their magmatic composition (Figure 15).

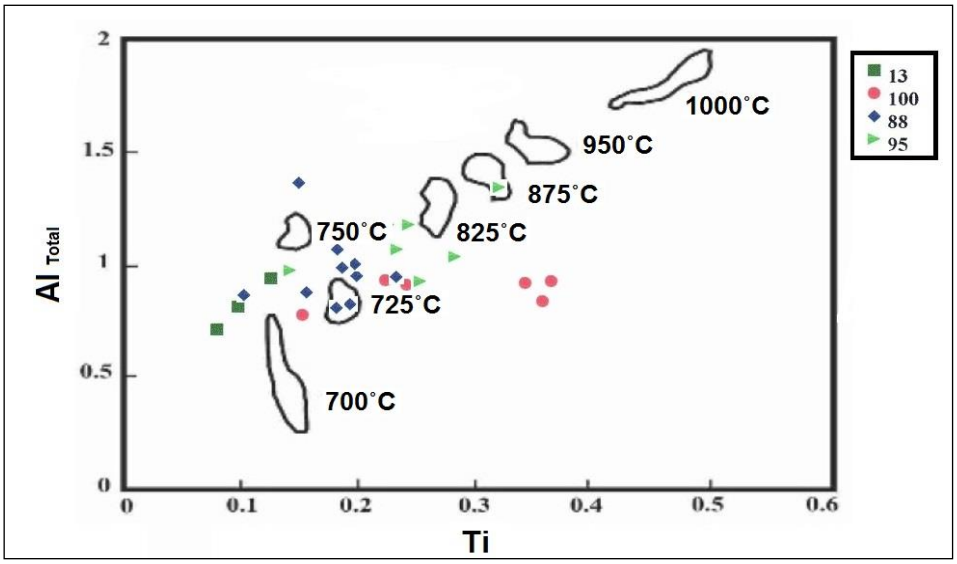

Figure 15: The approximate formation temperature of amphiboles.
Source: Helz (1993).

On the other hand, according to Al^{Total} versus Fe/Fe+Mg, a pressure range of less than 1 kbar and 0.5-1.5 kbar can be estimated respectively for quartz monzodiorite and monzodiorite hornblendes (Figure 16).

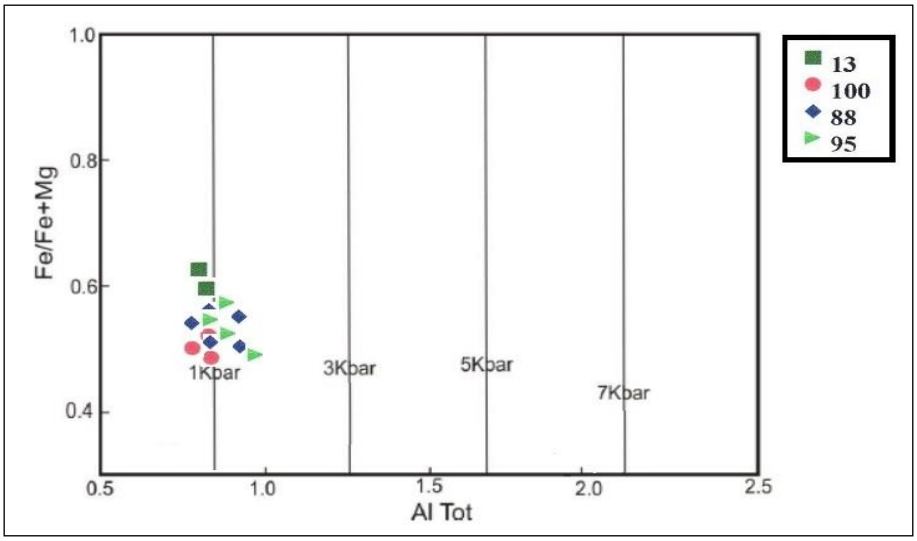

Figure 16. The approximate pressure calculated.
Source: Schmidt (1992).

The approximate temperature of the two rock units was estimated based on the pressure variations (in kbar) with Al^{Total} (Schmidt, Johanson ,1992). Accordingly, a

temperature ranges of 700 to 830 °C was estimated for quartz monzodiorite and 770 to 850 °C for monzogranite hornblendes (Figure 17).

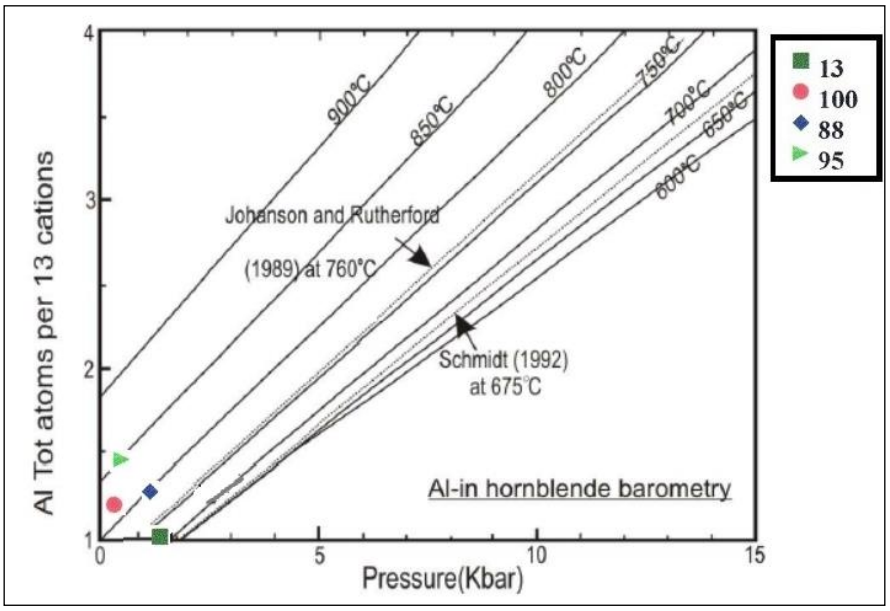

Figure 17. The temperature estimated.
Source: Schmidt (1992).

CONCLUSION

According to the electron microprobe analysis of plagioclases and amphiboles, the following results were obtained regarding the formation of the Shirkuh granitoid batholitic mass. In terms of magmatic series, the Shirkuh granitoid rocks are of the calc-alkaline type formed in a supra-subduction tectonic environment. All amphiboles in this complex have a magmatic origin and are categorized in the calcic and Fe-Mg-Mn amphibole groups. The oxidation and reduction of the magmatic origin of granitoids based on the amphibole composition are suggestive of high oxygen fugacity in the region. The thermometry of amphiboles showed a temperature range of 700-900 °C. The barometry by the Hammarstron and Zen (1986), Johnson, Rutherford (1989) Sehmidth (1992), Hollister and Grissorn (1987) and Helz (1993) methods indicated an average pressure of 0.8-1.5 kbar. Moreover, the

thermometry of feldspar by the Anderson (1997) method showed a temperature range of 770-900 °C.

ACKNOWLEDGMENTS

The authors would like to express their sincere gratitude to Dr. Afshin Ashja Ardalan for his assistance with this study.

REFERENCES

AGHANABATI, A. Major sedimentary and structural units of Iran. **Geosciences**, n**.** 7, Geological Survey of Iran: Tehran, 1998.

ALMEIDA, M. E.; MACAMBIRA, M. J. B.; OLIVEIRA, E. C. Geochemistry and zircon geochronology of the I-type High-K calk-alkaline and S-type granitoid rocks from southeastern Roraima, Brazil: Orosirian collisional magmatism evidence (1.97- 1.96 Ga) in central portion of Guyana Shield. **Precambrian Research,** 155, 2007. p. 69- 97.

ARSALAN, M.; ASLAN, Z. Mineralogy, petrography and whole-rock geochemistry of the Tertiary granitic intrusions in the Eastern Pontides, Turkey. **Journal of Asian Earth Sciences**, n. 27, 2006. p. 177-193.

AZ-MIKAELIANS, H.; ASHJA-ARDALAN, A.; SHEIKHZAKARIAYI, S.; ANSARI, S. H. Introducing the Main and Accessory Minerals in the Granitoid Batholith of Shirkuh, Yazd (Central Iran) and its Tourmaline and Garnet Phases: **Geosaberes**, v. 11, 2020. p. 76-99.

BARBARIN, B. A review of the relationships between granitoid types, their origins and their geodynamic environments. **Blackwell Oxford Lithos**, 46, 1999. p. 605- 626.

CHAPPELL, B. W.; WHITE, A. J. R. I-and S-type granites in the Lachlan fold belt. **Transactions of the Royal Society of Edinburgh Earth Sciences**, 83, 1992. p. 1-26.

CHAPPELL, B. W.; WHITE, A. J. R. Two contrasting granite types: 25 years later. **Australian Journal of Earth Sciences**, 48, 2001. 489-499.

CLARKE, D. B. **Granitoid rocks**. Chapman and Hall Publisher: London, 1992

DABIRI, RAHIM.; AKBARI-MOGADDAM, M.; GHAFFARI, M. Geochemical evolution and petrogenesis of the eocene Kashmar granitoid rocks, NE Iran: implications for fractional crystallization and crustal contamination processes, **Iranian Journal of Earth Sciences**, 10(1), 2018. p. 68-77.

DE LA ROCHE, H.; LETERRIER, J.; GRAND CLAUDE, P.; MARCHEL, M. A classification of volcanic and plutonic rocks using R1-R2 diagrams and major elements analysis-its relationship with current nomenclature. **Chemical Geology,** 29, 1990 p. 183-210.

DROOP, G. T. R. A general equation for estimating Fe3+ in ferromagnesian silicates and oxides from microprobe analysis, using stoichiometric criteria. **Mineralogical Magazine**, 51, 1987. p. 431 – 437.

ESMAEILI, E.; TABAKH SHABANI, A.; NAJJAR, H.; REZAEI, M. Using amphibole mineral chemistry in study of magmatic and producing characteristics and geothermobarometry of granitoidic plutons, NW of Saveh, Central Iran. **Iranian Journal of Crystallography and Mineralogy**, 21(3), 2013. p. 417-430 (in Persian).

FROST, B. R.; BARNES, C. G.; COLLINS, W. J.; ARCULUS, R. J.; ELLIS, D. J.; FROST, C. D. A geochemical classification for granitic rocks. **Journal of Petrology,** 42, 2001. p. 2033-2048.

HAJMOLLA ALI, A. **Geological map of Khezrabad 1:100000**, Series sheet 6753. Geological survey of Iran: Tehran, 1993. (in Persian).

HAJMOLLA ALI, A.; MAJIDIFAR M. R. **Geological map of Yazd 1:100000**. Geological survey of Iran: Tehran, 2000. (in Persian).

HARKER, A. The natural history of igneous rocks. Methuen: London, 1909.

HELMY, H. M.; AHMED, A. F.; EIMAHALLAWI, M. M.; ALI, S. M. Pressure, temperature and oxygen fugacity condition of calcalkaline Granitoids. Eastern Desert of Egypt and tectonic implication, **Journal of African Earth Sciences**, 38, 2004. p. 255- 268.

HOLLISTER, L. S. Confirmation of the empirical correlation of Al in hornblende with pressure of solidification of calcalkaline plutons. **American Mineralogists**, 72, 1987. p. 231-239.

HONARMAND, M.; AHMADIAN, J.; NABATIAN, G.; MURATA, M. Reconstructing physicochemical conditions by application of mineral chemistry: a case study from the Natanz pluton, Central Iran. **Neues Jahrbuch fur Mineralogy**, 189, 2012. p. 138 – 153.

JAMSHIDIBADR, M.; TARABI, S.; GHOLIZADEH, K. Study of micro-textures and chemistry of feldspar minerals of East Sarbisheh volcanic complex (Eastern Iran), for evidence of magma chamber process. **Iranian Journal of Earth Sciences**, 12(1) 2020. p. 10-31.

JANOUSEK FARROW, C. M.; ERBAN, V. **package "GCDKit**". Version 3.00, 2008

KHODAMI, M.; KAMALI SHERVEDANI, A. Mineralogical and geochemical characteristics of the Chah-Shur clay deposit, Southeast of Isfahan, Iran, **Iranian Journal of Earth Sciences**, 10(2), 2018. p. 135-141.

LAMEYRE, J.; BOWDEN, P. Plutonic rock types series: discrimination of various granitoid and related rocks. **Journal of Volcanology and Geothermal Research**, 14, 1982. p. 169-86.

LEAKE, B. E,. Nomenclature of amphiboles of the subcommittee on amphiboles of the international mineralogical association commission on new minerals and mineral names. **European Journal of Mineralogy**, 9, 1997. p. 623- 651.

MOAZZEN, M.; DROOP, G. T. R. Application of mineral thermometers and barometers to granitoid igneous rocks: The Etive Complex. **Mineralogy and Petrology**, 83, 2005. p. 27-53.

MOBASHERGERMI, M.; ZARAISAHAMIA, R.; AGHAZADEH, M.; AHMADIKHALAJI, A.; AHMADZADEH, G. H. Mineral chemistry and thermobarometry of Eocene alkaline volcanic rocks in SW Germi, NW Iran, **Iranian Journal of Earth Sciences**, 10 (1) 2018, p. 39-51.

NOVRUZOV, N.; VALIYEV, A.; BAYRAMOV, A.; MAMMADOV, S.; IBRAHIMOV, J.; EBDULREHIMLI, A.; () Mineral composition and paragenesis of altered and mineralized zones in the Gadir low sulfidation epithermal deposit (Lesser Caucasus, Azerbaijan), **Iranian Journal of Earth Sciences**, 11(1), 2019. p. 14-29.

PARADA, M. A.; NYSTROM, J. O.; LEVI, B. Multiple source for the Costal Batholith of Central Chile: geochemical a Sr- Nd isotopic evidence and tectonic implication. **Lithos**, 46, 1999. p. 505- 521.

PEARSE, J. Sources and setting granitic rocks. **Episodes**, 19 (4), 1996. p. 120-125.

PICHER, W. S. **The nature and origin of granite**. Chapman and Hall: London, 1995

RASOULI, J.; GHORBANI, M.; AHADNEJAD, V.. Field observation, Petrography and microstructures study of Jebal Barez Plutonic complex (East – North East Jiroft). **Journal of Tethys**, 2(3) 2014. p. 178- 195.

ROLLINSON, H. R. **Using geochemical data**: evaluation, presentation, interpretation. Longman: Harlow, 1993.

SCHMIDT, M. W. Amphibole compositon in tonalite as a function of pressure an experimental calibration of the Al – hornblende barometer. **Contribution to Mineralogy and Petrology**, n. 110. 1992. p. 304 – 310.

SHELLEY, D. Hgneouse and metamorphic rocks under the microscope, classification, textures, microstructures and mineral preferred- orientations. **Chapman and Hall**: London, 1993.

SUTCLIFFE, R. H.; SMITH, A. R.; DOHERTY, W.; BARNET, R. I. Mantel derivation of Archean amphibole- bearing granitoid and associated mafic rocks: evidence from the southern superior province, Canada. **Mineralogy and Petrology**, 105, 1990. p. 255-274.

WHITE, A. J. R.; CHAPPLE, B. W. Granitoid types and their distribution in the Lachlan Fold Belt, southeastern Australia. **Geological Society American Memory**, n. 159, 1983. p. 21- 34.

XIE, Y. W.; ZHANG, Y. Q. Peculiarities and genetic significance of hornblende from granitic in the Hengduansan region. **Acta Mineral Sin** (in Chinese), 10, 1990. p. 35-45.

YAZDI, A.; ASHJA-ARDALAN, A.; EMAMI, M.H.; DABIRI, R.; FOUDAZI, M. (). Chemistry of Minerals and Geothermobarometry of Volcanic Rocks in the Region Located in Southeast of Bam, Kerman Province. **Open Journal of Geology**, 7, 2017. p. 1644-1653.

YAZDI, A.; ASHJA ARDALAN, A.; EMAMI, M.H.; DABIRI, R.; FOUDAZI, M. Magmatic interactions as recorded in plagioclase phenocrysts of quaternary volcanics in SE Bam (SE Iran), **Iranian Journal of Earth Sciences**, 11(3), 2019. p. 215-225.